Potential of salivary gland stem cells in regenerative medicine

Maimets, Martti

CHAPTER 6

HUMAN SALIVARY GLAND STEM CELLS FUNCTIONALLY RESTORE RADIATION DAMAGED SALIVARY GLANDS

Pringle, S., Maimets, M., van der Zwaag, M., Stokman, MA., van Gosliga, D., Zwart, E., Witjes, MJH., de Haan, G., van Os, R., Coppes, RP.

Stem Cells. 2016 Mar;34(3):640-52.

ABSTRACT

Adult stem cells are often touted as therapeutic agents in the regenerative medicine field, however data detailing both the engraftment and functional capabilities of solid tissue derived human adult epithelial stem cells is scarce. Here we show the isolation of adult human salivary gland (SG) stem/progenitor cells and demonstrate at the single cell level in vitro self-renewal and differentiation into multilineage organoids. We also show in vivo functionality, long-term engraftment, and functional restoration in a xenotransplantation model. Indeed, transplanted human salisphere-derived cells restored saliva production and greatly improved the regenerative potential of irradiated SGs. Further selection for c-Kit expression enriched for cells with enhanced regenerative potencies. Interestingly, interaction of transplanted cells with the recipient SG may also be involved in functional recovery. Thus, we show for the first time that salispheres cultured from human SGs contain stem/progenitor cells capable of self-renewal and differentiation and rescue of saliva production. Our study underpins the therapeutic promise of salisphere cell therapy for the treatment of xerostomia.

INTRODUCTION

The salivary glands (SGs) are exocrine organs whose parenchymal tissue manufactures and secretes saliva. Rat submandibular SG duct ligation induces dysfunction/atrophy of saliva-producing acinar cells, and rapid diminishment of saliva production, while ductal cells remained unharmed. Upon de-ligation, proliferation and differentiation of these ductal cells into acinar cells was observed, and saliva flow rather rapidly returned to pre-ligation levels, indicating the pronounced regenerative potential of SGs (Cotroneo et al., 2010; Cotroneo et al., 2008; Katsumata et al., 2009; Osailan et al., 2006; Takahashi et al., 2004). Label retaining cell studies hinted at the presence of putative stem/pro- genitor cell populations residing in the ducts of rodent SGs (Denny et al., 1993) and indicated that SGs are "slow-turnover" in nature, as opposed to "fast- turnover" tissues such as intestines. These data imply that SGs harbor a resident stem or progenitor cell population that is capable of regenerating the parenchyma of the SG. Studies using a malleable mouse embryonic SG model to study branching morphogenesis have identified populations of embryonic SG stem cells, defined both by their keratin-5 expression and reliance on nervous stimulation for maintenance (Knox et al., 2013; Knox et al., 2010). Numerous studies in adult SG models have now demonstrated isolation and culture of stem/progenitor-like cultures from rodent SGs. Using a variety of culture techniques, these studies suggest rodent SG stem/progenitor cells express well-established stem cell surface marker proteins such as CD24 (Nanduri et al., 2011), CD29 (David et al., 2008; Nanduri et al., 2011; Neumann et al., 2012), CD49f (David et al., 2008; Nanduri et al., 2011; Neumann et al., 2012), CD117/c-kit (Banh et al., 2011; Lombaert et al., 2008a; Neumann et al., 2012), clusterin (Mishima et al., 2012), Sca-1 (Mishima et al., 2012), and Ascl3 (Rugel-Stahl et al., 2012). Murine SG stem/progenitor cells have been shown to be capable of in vitro expansion and differentiation into parenchymal acinar- and duct-like cell lineages (Banh et al., 2011; Kishi et al., 2006; Lombaert et al., 2008a; Maimets et al., 2016; Nanduri et al., 2014; Neumann et al., 2012; Rugel-Stahl et al., 2012). Interestingly, the nascent regenerative potential of murine salisphere derived cells was enhanced upon selection of a $CD24^{hi}CD29^{hi}$ subset, associated with stem/progenitor cells in other tissues (Shackleton et al., 2006). These $CD24^{hi}CD29^{hi}$ salisphere cells showed pronounced self-renewal abilities indicated by high potential to form secondary salispheres and to differentiate into organoids containing both ductal and acinar cell lineages (Nanduri et al., 2014). Similarly, $CD24^{+}$c-$Kit^{+}Sca\text{-}1^{+}$ murine salisphere cells also demonstrated greater salisphere-formation potential than their non-marker expressing counterparts in a separate study (Xiao et al., 2014). In vivo functionality of murine SG stem/progenitor cells has been repeatedly demonstrated, whereby as few as 100 CD117/c-kit^{+} cells (Lombaert et al., 2008a), 300 $CD24^{+}$c-$Kit^{+}Sca\text{-}1^{+}$ cells (Xiao et al., 2014), or 10,000 culture-enriched $CD24^{hi}CD29^{hi}$ murine SG stem progenitor cells (Nanduri et al., 2014) rescued radiation-

induced hyposalivation in a mouse model. All three stem/progenitor cell phenotypes showed integration into the recipient SG and displayed ductal and acinar cell-type morphologies (Lombaert et al., 2008a; Nanduri et al., 2014; Xiao et al., 2014).

These data demonstrate the potential clinical utility of SG stem/progenitor cells as a novel therapeutic strategy to treat SG dysfunction. Hyposalivation, and its collection of associated ailments, resulting in xerostomia, is observed in 40% of patients receiving unavoidable radiation of the SGs during head and neck cancer therapy. Reduction in saliva production is immediate, irreversible, and impacts greatly on patient quality of life. Hyposalivation leaves in its wake life-long oral, dental, speaking, eating and sleeping problems, which have no current cure (Burlage et al., 2001; Vissink et al., 2003a; Vissink et al., 2003b). New therapies for xerostomia therefore represent an unmet clinical need. Although stem cells have been isolated from several adult human tissues such as bone marrow, brain, eye, dental pulp, intestine, adipose tissue, lung, skin and muscle (Baglioni et al., 2009; Jones and Watt, 1993; Kajstura et al., 2011; Kaukua et al., 2014; Marg et al., 2014; Ohyama et al., 2006; Pellegrini et al., 1997; Reynolds and Weiss, 1992; Sato and Clevers, 2013), very little is known about human SG stem or progenitor cells. Preliminary studies of cultures of various formats from human SGs have indicated expression of surface proteins CD44 (Maria et al., 2012), CD24 (Pringle et al., 2013), CD29 (Pringle et al., 2013), CD49f (Sato et al., 2007), CD117 (Feng et al., 2009; Lombaert et al., 2008a; Pringle et al., 2013), CD133 (Pringle et al., 2013), CD90 (Banh et al., 2011), CD34 (Cotroneo et al., 2008), CD166 (Maria et al., 2012) and aldehyde dehydrogenase (Banh et al., 2011), similar but not the same to what has been shown in the rodent SG, and with limited examination of in vitro differentiation potential of human salispheres (Feng et al., 2009; Pringle et al., 2013). To date there has been no exploration of the engraftment capabilities or functional attributes of human SG stem/progenitor cells. Therefore, we present in this study the first data exploring the potential of human SG stem/progenitor cells, including their self-renewal and differentiation properties and in vivo engraftment and functionality. Our results pave the way for the development of a cell therapy for xerostomia.

MATERIALS AND METHODS

Source of SG Tissue

Human non-malignant submandibular SG tissue was obtained from donors (after informed consent and IRB approval) with a squamous cell carcinoma of the oral cavity, in whom an elective head and neck dissection procedure is performed. During this procedure submandibular SG is exposed and

removed as part of the dissection procedure. This cohort represents the patient group most eligible for stem cell transplantation, following clinical translation.

Salisphere Cultures

Submandibular SG biopsies were collected after surgery into Hank's Balanced Salt Solution (HBSS) containing 1% bovine serum albumin (BSA; Invitrogen, Carlsbad, CA, http://www.invi- trogen.com). Biopsies were mechanically digested using the gentleMACS dissociator (Miltenyi Biotec, Bergisch Gladbach, Germany, http://www.miltenyibiotec.com) and simultaneously subjected to digestion in HBSS/1% BSA buffer containing 0.63 mg/mL collagenase II (Invitrogen) and 0.5 mg/mL hyaluronidase (Sigma Aldrich, St. Louis, MO, https://www.sigmaaldrich. com), and calcium chloride at a final concentration of 6.25 mM, for two periods of 30 minutes at 37°C. Twenty mg of tissue was processed per 1 mL buffer volume, total volume was adjusted according to biopsy weight. Digested cells were collected by centrifugation, washed twice in HBSS/1% BSA solution, and passed through 100 μm cell strainers (BD Biosciences, San Diego, http://www.bdbiosciences.com). Resultant cell suspensions were collected again by centrifugation and re-suspended in Dulbecco's modified Eagle's medium:F12 medium containing Pen/Strep antibiotics (Invitrogen), Glutamax (Invitrogen), 20 ng/mL epidermal growth factor (EGF) (Sigma Aldrich, https://www.sigmaaldrich.com/), 20 ng/mL fibroblast growth factor-2 (Sigma), N2 (Invitrogen), 10 μg/mL insulin (Sigma), and 1 μM dexamethasone (Sigma), and plated at a density of 400,000 cells per well of a 12-well plate. For salisphere culture from mouse SG, both submandibular glands from a single mouse were digested in a 2 mL volume of the same hyaluronidase/collagenase buffer solution and processed otherwise in the same manner as human tissue.

Self-Renewal Assay

Salisphere cultures of 3–5 day (d) were dispersed to form single cell suspensions using 0.05% trypsin-EDTA (Invitrogen), enumerated, and concentration adjusted to 0.4 x 10^6 cells per mL. 25 μL of this cell solution was combined on ice with 50 mL volumes of Basement Membrane Matrigel (BD Biosciences, Franklin Lakes, NJ, https://www.bdbiosciences.com) and deposited in the center of 12-well tissue culture plates. After solidifying the Matrigel for 20 minutes at 37°C, gels were covered in salisphere medium as defined above. New spheres appeared 2–3 days post seeding of single cells in Matrigel. One week after seeding, Matrigel was dissolved by incubation with Dispase enzyme (1mg/mL for 30 minutes to 1 hour at 37°C; Sigma). Spheres released from the gels were processed to a single cell suspension using 0.05% trypsin-EDTA, cell number and sphere number noted, and encapsulation in Matrigel repeated. This cycle was repeated up to five times (5 passages). Cell numbers seeded at the start of each passage and harvested at the end were used to calculate the

number of population doublings that had occurred, using the following formula, where PD = population doublings and ln = natural log.

$$pd = \frac{ln\ (harvested\ cells\ /\ seeded\ cells)}{ln2}$$

For time-lapse microscopy, single cells were seeded as described, and imaged every hour for 96 hours, using the Zeiss 780 confocal inverted microscope.

Organoid Differentiation

Single cell-derived salispheres were encapsulated in a three- dimensional matrix consisting of a 60:40 ratio of Type I rat tail collagen to growth factor reduced Matrigel (BD Biosciences). After solidifying the gel at 37°C for 20 minutes, salisphere medium containing 10% fetal calf serum (FCS, Invitrogen) was added and cultures maintained for up to 3 weeks.

Immunostaining

Organoids were removed from plate and fixed in 4% formaldehyde (FA; 20 minutes, 4°C), before washing, embedding in paraffin wax, and processing to 5 µm sections. Transplanted murine SGs were either snap-frozen in liquid nitrogen, stored at -80°C and processed to 8 µm cryostat sections or FA fixed [24 hours, room temperature (RT)], and processed for paraffin sections. After air drying, frozen sections were fixed in 4% FA (10 minutes, RT), and washed with phosphate buffered saline (PBS). Hematoxylin and Eosin staining was performed according to standard protocols. For PKH26 cell-tracing, nuclear counterstaining with 0.2mg/mL 40,6-diamidino-2-phenylindole (DAPI; 10 minutes, RT) was performed, and sections visualized in the phycoerythrin-fluorescence channel. An average of 100 slides per SG were cut, and PKH26 screening performed every 10 slides. For immunohistological analysis of frozen tissues, relevant primary antibodies were added to fixed tissue in PBS (2 hrs, RT), washed thrice with PBS, incubated with secondary antibodies (1hr, RT) and counterstained with DAPI as above. Dilutions of primary antibodies used for immunostaining of frozen sections were: mouse anti-human nuclei (1:50, Chemicon, Temecula, CA, http://www.chemicon.com; clone 235-1); mouse anti-cytokeratins (1:00, Abcam, Cambridge, U.K., http://www.abcam.com; clone AE1/AE3); rabbit anti-human α-amylase (1:100, Sigma, polyclonal); rabbit anti-aquaporin-5 (1:100, Abcam polyclonal). Secondary antibodies were goat anti-mouse-Alexafluor-488 or goat anti-rabbit-Alexafluor-594 conjugates, used at 1:300 dilutions. Fluorescent stainings were visualized using the Leica 6000 series microscope or the Leica TCS SP8 confocal laser scanning microscope and Leica Application Suite software. For immunostaining on paraffin wax- embedded human submandibular gland sections and

transplanted glands, sections were boiled for 10 minutes in preheated 10 mM sodium citrate buffer (pH 6.0) containing 0.05% Tween 20 and washed prior to primary antibody exposure. No antigen retrieval was necessary for organoid sections. Dilutions of primary antibodies for paraffin-section immunostainings were: rabbit anti-mouse Ki67 (1:100, Cell Marque); rabbit-anti mouse fibronectin (1:500, Millipore, Billerica, MA, http://www.millipore.com), mouse anti-mouse b-catenin (1:100, BD Laboratories). Secondary conjugates as above; nuclear counterstaining was performed with DRAQ5 (1:1,000, BD Laboratories).

Masson's Trichrome Staining

Tissue sections of 5 lm were incubated in Erhlich's Hematoxylin for 5 minutes and rinsed in tap water. Sections were then incubated for 5 minutes in a 2:1 ratio of 1% (w/v) acid fuschien (Sigma Aldrich) in 1% (v/v) glacial acetic acid (aq) with 1% Ponceau Xylidine (Sigma Aldrich) in 3% glacial acetic acid (aq). After washing in deionized water, sections were incubated for 1 minute in 1 % Aniline Blue (Klinipath, Duiven, Netherlands, http://www.klinipath.nl) in 3% glacial acetic acid (aq), washed in deionized water, and finally incubated for 5 minutes in 1 % (w/v) molybdenum phosphoric acid (aq) (Alfa Aesar, Halverville, MA, https://www.alfa.com) and washed again. Sections were dehydrated and mounted as standard.

Quantitative Polymerase Chain Reaction

Genomic DNA was extracted from human salisphere-transplanted SGs at relevant time points, using the Qiagen DNeasy Blood and Tissue kit and adjusted to a concentration of 5mg/mL (Qiagen, Valencia, CA, https://www.qiagen.com/gb). Total RNA was extracted using the Qiagen RNeasy Minikit. For cDNA generation, 1mg of total RNA was reverse transcribed using 0.5 mg oligo(dT)15–18 primers, 0.5 mM dNTPs, 13First-strand Buffer, 0.01M dithiothreitol, 400 U RnaseOut, and 200 U of M-MLV Reverse Transcriptase (all Invitrogen), in a total volume of 20 µL per reaction. Quantitative polymerase chain reaction (Bio-Rad, Hercules, CA, http://www.bio-rad. com) (qPCR) was performed using Bio-Rad iQ SYBR Green Supermix according to manufacturer's instruction, primers at a final concentration of 1.67µM and 25ng load of genomic DNA or cDNA per reaction. Primer sequences are listed in Supplementary Information Table S1. For detection of human mitochondrial DNA, a standard curve was generated using a dilution series of human genomic DNA in mouse genomic DNA, with a constant load of 25ng DNA per qPCR reaction. A two-step qPCR reaction using the Bio-Rad iCycler was used to amplify human mitochondrial DNA, and approximate proportion of human cells in transplanted glands inferred from standard curve.

Irradiation, Cell Transplantation, and Saliva Collection of/into/from Mouse SG

All mice were housed in individually ventilated cages and in accordance with the Wet op de dierproeven (1977). Mice were fed ad libitum. SGs of NOD.C*g-Prkdc*^{scid}*Il2rg*^{tmlWjl}/SzJ (NSG) mice were locally irradiated with a single X-ray dose of 5 Gy under isofluorane anesthesia. This dose ablated function of SGs without compromising general health of the animals. Cell transplantation was performed 1 month following irradiation. Cultures of human salispheres between 3 and 5 days post-isolation were trypsinized to single cell suspensions using 0.05% trypsin-EDTA and labeled with PKH26 Red Fluorescent Cell Linker Kit (Sigma). Upon cell proliferation, the intensity of the PKH26 labeling is halved; hence PKH26-mediated fluorescence indicates proliferative abilities of the cells. Following labeling, cells were suspended in a 5µL volume of alpha- modified eagle's medium with 2% FCS. For transplantation, a 5 mm incision was made in the neck of NSG mice under iso- fluorane anesthesia and the submandibular SG exposed. 500, 5,000, or 50,000 human salisphere cells per gland were injected into the submandibular SG, where after the wounds were closed by suturing. At 1, 2, and 3 months post- irradiation, whole stimulated saliva was collected from trans- planted and control animals. Two mg/kg pilocarpine was administered subcutaneously to the animals, and saliva collected by suction pump for 15 minutes. The quantity of saliva was determined gravimetrically, assuming a density of 1g/mL saliva and normalized to the weight of the animal and pre- irradiation saliva flow rate.

Genome-Wide Expression Analysis

Genome-wide gene expression was profiled in NSG submandibular SGs transplanted with 100,000 human or autologous NSG salisphere cells per animal, at 1 week post- transplantation. Time-matched irradiated controls were used to eliminate effects of radiation on the transcriptome. Samples were analyzed in triplicate. Total RNA was isolated using the RNeasy Mini Kit. Highly pure total RNA (300ng/sample) was used for expression profiling on Illumina WG6v2.0 expression bead chip kit. RNA was amplified using the Illu- mina TotalPrep RNA Amplification Kit (Ambion, Austin, TX, http://www.ambion.com/Applied Biosystems, Foster City, CA, http://www.appliedbiosystems.com) and hybridized to Sentrix MouseWG-6 Version 2.0 expression beadchips (Illumina, San Diego, CA, www.illumina.com) according to the manufacturer's instructions. Hybridization and washing were performed by in-house Genome Analysis Facility (University Medical Centre Groningen). Scanning was carried out on the iScan System (Illumina). Data were extracted using GenomeStudio software (Illumina). The data were normalized using the R version 3.0.1 neqc function of the BioConductor version 2.12 library limma 3.16.5 (Smyth et al., 2005) by control background correction, quantile normalization, and log2 transformation and batch effects between arrays. Differential expression

analysis was performed using eBayes function of the BioConductor library limma and an adjustment method BH (Benjamini Hochberg) to exclude false positives, with a *p* value of .05. Assignment of probes upregulated at 1 week post-transplantation to bio- logical pathways was performed using ENrichR online resources (http://amp.pharm.mssm.edu/Enrichr/).

Statistical Analysis

A two-way ANOVA and Bonferroni post hoc test with α values of 0.05 were applied to the time course analysis of saliva flow. *n* numbers for tested groups are stated in figure legend. A non-parametric one-way ANOVA (Kruskal Wallis test) and Dunn's post hoc testing with α values of 0.05 was applied to qPCR data in Figure 4. Additional methods for supplementary figures can be found in Supplementary Information file.

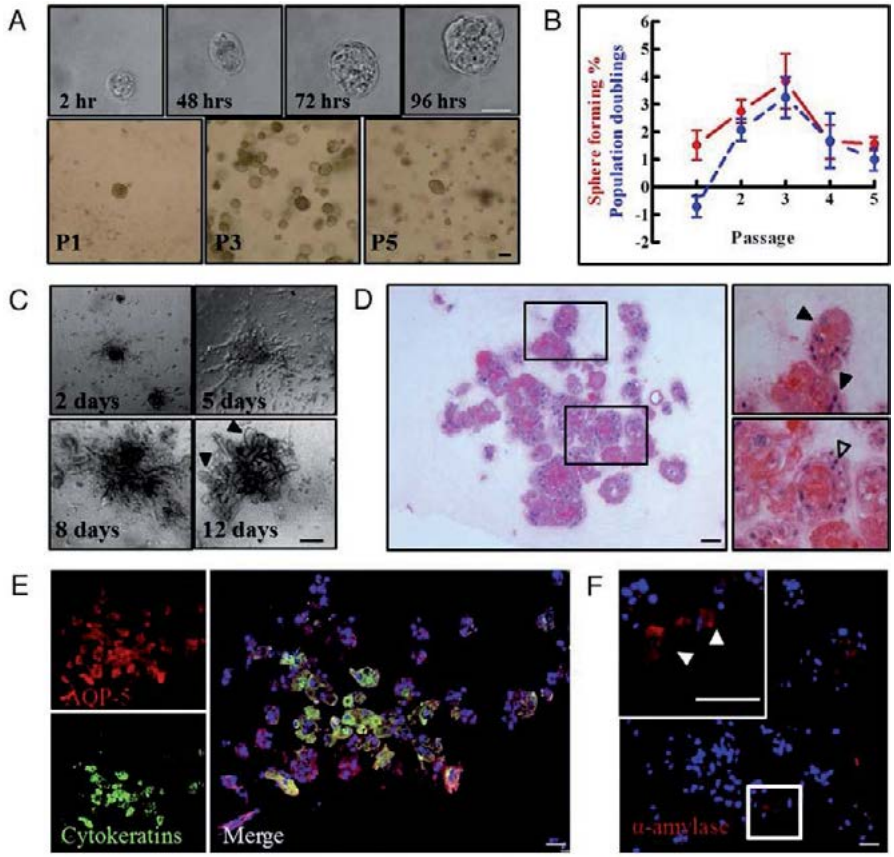

Figure 1 Human salispheres have self-renewal capacity, can be expanded in vitro, and are bipotent. **(A)**: Still frame images from time lapse microscopy of a human salisphere increasing in size in culture, time indicated in each still frame image (upper row) and phase contrast microscopy of salisphere

self-renewal cultures at passages 1, 3, and 5 (lower row). Scale bars = 10 μm and 100 μm for upper and lower rows, respectively. **(B)**: Population dynamics of salisphere self-renewal cultures. Population doublings (formula in Materials and Methods section) and percentage of salisphere-forming cells (as percentage relative to input cell number) were calculated at the end of each passage. Data points are means and SEM and are derived from a minimum of 3 and maximum of 10 separate donor isolations per passage. **(C)**: Phase contrast microscopy of differentiating single cell-derived human salispheres at 2, 5, 8, and 12 days of organoid culture in differentiation conditions. **(D)**: Hematoxylin and eosin staining of an organoid following 12 days of differentiation, depicting putative ductal and acinar-like structures. High-resolution images correspond to black boxes inset in low resolution panel. **(E)**: Cytokeratin and AQP-5 immunostaining of organoids following 12 days in differentiation shows central localization of cytokeratin^{+} putative ductal cells and peripheral localization of a second AQP-5^{+} cytokeratin^{-} cell type. **(F)**: α-Amylase expression in peripheral cells of 12-day organoids. Empty arrows denote duct-like tubular structures; solid arrows denote acinar cell-like spherical structures or cells, in all panels. Scale bars = 50 μm (C–F). Abbreviation: AQP-5, aquaporin-5.

RESULTS

Single Cell-Derived In Vitro Self-Renewal and Organoid Formation from Human SG Stem Cells

Human salispheres were cultured from healthy human SG biopsies according to an optimized previously published protocol (Feng et al., 2009). Primary human salispheres cultured from such mechanically and enzymatically dissociated human submandibular (SG) biopsies grew in size over time (Fig. 1A), in a similar manner to those from the mouse (Lombaert et al., 2008a; Nanduri et al., 2014). These cells were actively dividing as indicated by abundant expression of proliferating cell nuclear antigen (Supplementary Information Fig. S1A, S1B). Culturing primary human salispheres did not induce karyotypic abnormalities, as demonstrated by karyotype spread analysis (Supplementary Information Fig. S2).

To determine whether human salispheres contain stem/pro- genitors, in vitro self-renewal and differentiation potential was assessed. When primary human salispheres were enzymatically dispersed into single cells, they were able to form secondary human salispheres in a 3D matrix (Fig. 1A; Supplementary Information Video 1). Moreover, this procedure could be repeated for at least 5 passages and up to 10 passages in some cases, indicating extensive self-renewal potential. The maximum salisphere cloning frequency was 4.37% 6 1.09% SEM at passage 3 (Fig. 1A, 1B). When self-renewal potential declines, we observed an increase in apoptotic cells (Supplementary Information Fig. S3), indicating that our culture conditions are not optimal yet for long-term in vitro self-renewal. Thus, human salispheres derived from clinical biopsies contain cells that are able to self-renew in vitro at the single cell level. To evaluate the potential of human salisphere cells to generate functionally mature SG cell lineages, we performed in vitro differentiation studies. Some differentiation into mucin producing acinar cells was observed in salispheres themselves

(Supplementary Information Fig. S1C), but transferring single cell-derived human salispheres to a Matrigel/collagen matrix induced formation of organoids with SG structures, with branching occurring as early as 2 days after transfer (Fig. 1C). After 12 days, complex structures developed which contained both branching and lobular structures (Fig. 1C, 1D). Moreover, branches expressed the ductal cell marker Cytokeratin (Fig. 1E; Supplementary Information Fig. S4) while lobular structures expressed α-amylase (Fig. 1F; Supplementary Information Fig. S4), and aquaporin-5 (AQP-5; Fig. 1E), a water channel protein expressed in the apical membrane of acinar cells, indicative of differentiation into multiple SG lineages. Collectively, the in vitro data demonstrate that human salispheres contain stem/progenitor cells capable of both self-renewal and multilineage differentiation.

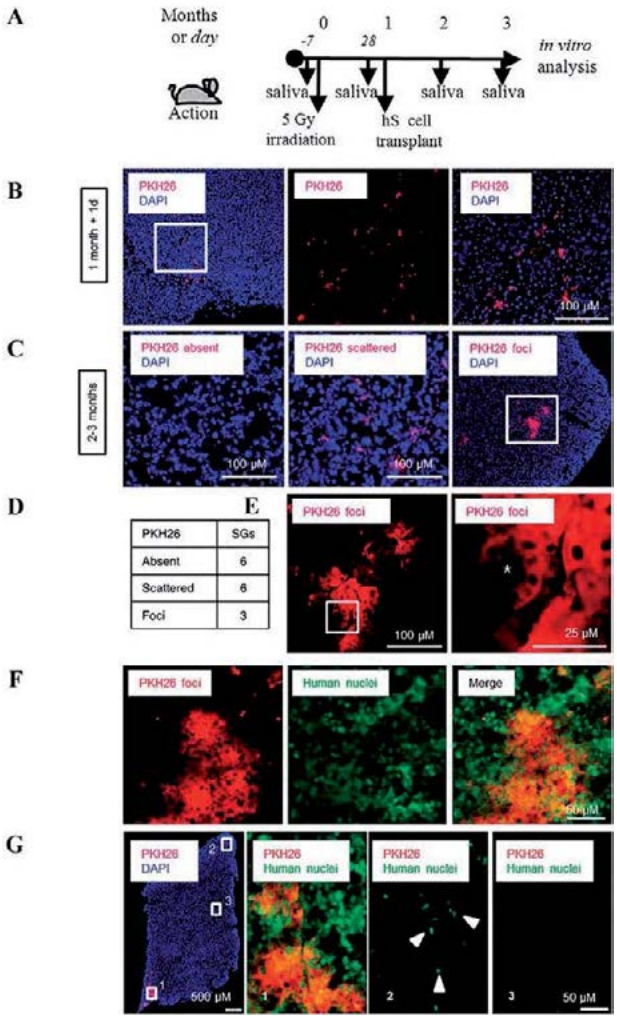

Figure 2. Transplanted human salisphere (hS) cells proliferate in the irradiated mouse SG. **(A)**: Scheme of workflow. **(B)**: hS cells visualized using the PKH26 label at 1 day post-SG transplantation (1 month + 1 day post-irradiation). At 2 months post-irradiation, $PKH26^+$ cells were either not observed, detected as scattered cells, or detected as organized foci (**C**, summarized in **D**). **(E)**: When $PKH26^+$ foci were observed, dilution of the PKH26 label could be seen, indicative of proliferation of human salisphere cells. High resolution microscopy of white-boxed inset areas are shown. *Marks $PKH26^+$ putative duct structure. **(F)**: Colocalization of anti-human nuclei (AHN) immunostaining with PKH26 label 2 months post-irradiation. **(G)**: AHN immunostaining and correlation with PKH26 foci at different sites within a human salisphere transplanted gland. Numbers 1–3 correspond to boxed numbered regions in first panel. Scale bars = 100 μm (B, C, and E) and 25 μm (high resolution E). Scale bars = 50 μm, 500 μm, and 50 μm (in F and G, respectively). Nuclei counterstained with DAPI where applicable. Abbreviations: DAPI, 40,6-diamidino-2-phenylindole; SG, salivary gland.

In Vivo Proliferation and Differentiation of Human Salisphere Cells

Next we investigated the regenerative potential of human salisphere cells in vivo. Immune-deficient NOD/SCIDIL2Rg$^{-/-}$ (NSG) mice were locally irradiated with 5 Gy in the neck region. After 1 month, mice received intra-submandibular SG transplantations of 500, 5,000, or 50,000 enzymatically dispersed human salisphere cells per gland, isolated from 3–5 day cultured primary human salisphere cells. Both glands in each mouse received equal cell numbers, so that a total cell number of 1,000, 10,000, or 100,000 cells were transplanted per recipient mouse. At least seven animals per group were transplanted with human salisphere cells obtained from at least three donors, which were transplanted separately (see scheme in Fig. 2A). Prior to transplantation human salisphere cells were labeled with the PKH26 fluorescent cell membrane dye allowing visualization of donor cells after transplantation (Supplementary Information Fig. S5A). $PKH26^+$ cells were found scattered throughout the gland 1 day after injection (Fig. 2B). Injection of PKH26 alone did not result in labeling of the SG (Supplementary Information Fig. S5B). At 2–3 months post-irradiation, scattered cells and foci of PKH26-labelled cells could be observed, with a peripheral dilution of PKH26-labelling intensity (Fig. 2C, 2D), indicating proliferation of the transplanted cells. Within $PKH26^+$ foci, duct-like arrangements of $PKH26^+$ cells were present, suggesting cellular organization into functional units (Fig. 2E). Immunostaining with an antibody specific to human nuclei revealed co-localization with $PKH26^+$ foci, confirming that $PKH26^+$ cells are transplanted human salisphere cells (Fig. 2F, for specificity see Supplementary Information Fig. S6). Immunostaining with a human specific antibody against major histocompatibility complex (MHC) Class I confirmed the differentiation of transplanted cells in ductal and acinar cell arrangements (Supplementary Information Fig. S5C). Human cells were also detected beyond PKH26 foci, indicating that the label was diluted below the detection threshold (Fig. 2G). Quantification of $PKH26^+$ foci revealed that 12% ± 7% and 36% ± 8% of foci cells displayed recognizable ductal (rectangular narrow shape, arrangement around lumen) or acinar (triangular shape with basally located nucleus) cell morphologies, respectively (Fig. 3A–3C; Supplementary

Information Fig. S5D). Quantification of MHC Class I labeled cells mirrored this distribution (4% ± 5% ductal and 10% ± 8% acinar cells, Supplementary Information Fig. S5E). Having established that PKH26^{+} cells are transplanted human cells with an ability to form organized structures, we then examined expression of marker proteins associated with the functional human SG. Differentiation of the transplanted cells into functionally mature tissue in the recipient gland was indicated by the co-localization of α-amylase, AQP-5, and cytokeratins with, or in close proximity to, PKH26^{+} cells (Fig. 3,

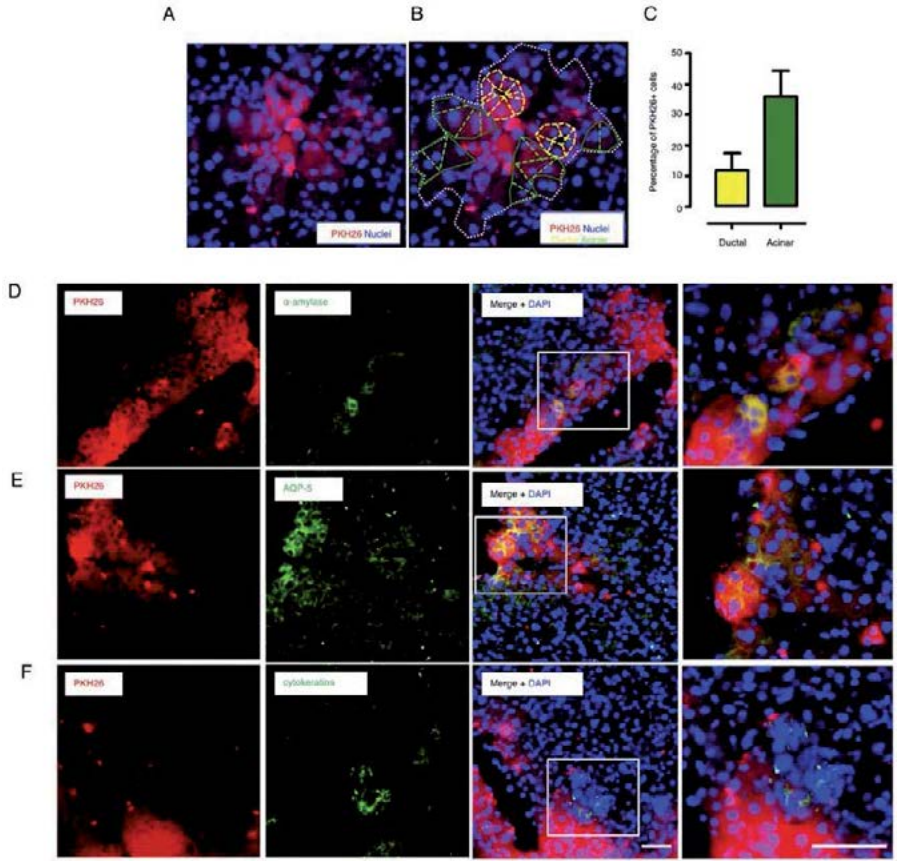

Figure 3. Transplanted human salisphere cells differentiate and express proteins associated with the human salivary gland in the irradiated mouse salivary gland. **(A–C)**: Representative images of acinar and ductal-like cells quantification in PKH26^{+} foci. (A) PKH26^{+} foci and (B) same PKH26^{+} as analyzed for acinar (yellow line) and ductal (green line) cells presence. Boundaries of analyzed foci are denoted with a white dashed line. (C): Quantification of proportion of acinar- and ductal-like cells in PKH26^{+} foci. PKH2^{+} foci at three depths within each transplanted glands were analyzed, from a total of three separate transplanted glands. Scale bars = SEM. **(D–F)**: Immunostaining for the acinar cell marker proteins (D) α-amylase, (E) AQP-5, and (F) ductal cell-associated proteins cytokeratins colocalizes with or is in close proximity to PKH26^{+} foci in cryostat sections of recipient gland, 2 months post-irradiation. White boxed insets are shown in high resolution. Scale bars = 50 µm. Abbreviations: AQP-5, aquaporin 5; DAPI, 40,6-diamidino-2-phenylindole.

for specificity of antibodies see Supplementary Information Fig. S4). These in vivo data demonstrate that human salisphere derived cells are capable of proliferation, differentiation, and long-term engraftment after xenotransplantation into an irradiated environment.

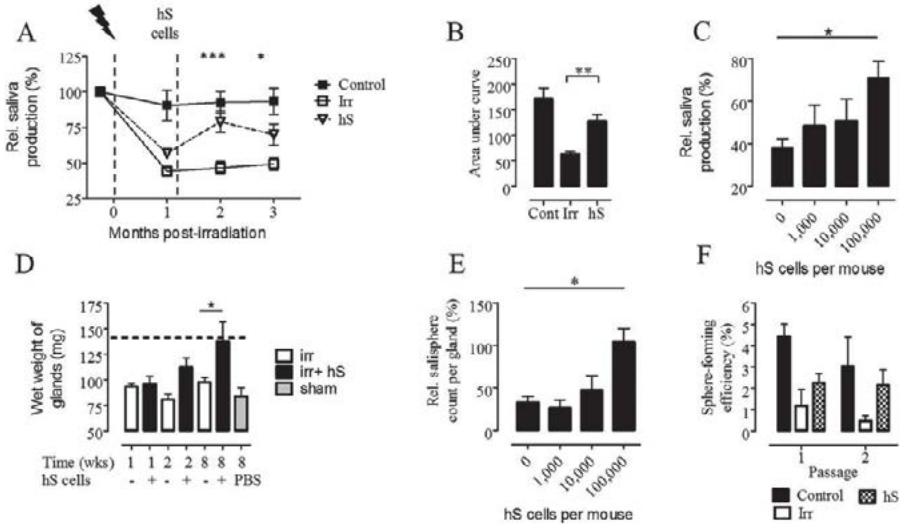

Figure 4. Transplanted hS cells are capable of rescuing radiation-induced hyposalivation and salisphere count, in a mouse model. **(A)**: hS transplants in time course analysis of relative saliva production, in comparison to control and irradiated control animals Statistical analysis is shown in comparison to irradiated control group (***, p<.001; *, p<.05 at relevant time point. n≥18 animals per time point in hS group and ≥9 for control groups. Scale bars = SEM. **(B)**: Area under the curve analysis of saliva flow data in (A), **, p < .01, Student's t test. Scale bars = SEM. **(C)**: Relative saliva production in animals transplanted with 100, 10,000, or 100,000 hS cells per mouse, compared to non-transplanted, irradiated animals ("0" group). Data are normalized to animal weight. Scale bars = SEM. n≥7 mice per group. *, p<.05, Student's t test. **(D)**: Wet weights of submandibular salivary glands (SGs from irradiated (irr), irradiated- transplanted (irr+hS), and sham-transplanted (sham) mice at 1, 2, and 8 weeks following irradiation. Transplanted mice received 100,000 human salisphere cells per animal. n≥3 mice per control and sham groups and n≥10 for hS transplanted groups. *, p<.05, Student's t test. **(E)**: Salisphere cultures from mouse SGs transplanted with 1,000, 10,000, or 100,000 hS cells per gland harvested at three months post-irradiation and compared to age-matched nontransplanted, irradiated control group ("0"). Scale bars = SEM. n≥7 mice per group. *, p<.05, Student's t test. **(F)**: Self-renewal assay using mouse SGs transplanted with 100,000 hS cells per animal, harvested 3 months post-irradiation. n = 9 animals in transplant group, n = 4 and 5 in control and irradiated control groups, respectively. Error bars represent SD.

Rescue of Hyposalivation by Human Salisphere Cells

To assess the functionality of the transplanted human salisphere cells, we determined pilocarpine stimulated whole saliva flow rate in the transplanted animals (Fig. 2A). In irradiated non-transplanted

animals saliva production dropped to 46% ± 4% of pre-irradiation values and was further maintained at 49% ± 4% at 3 months post-irradiation. Mice receiving sham transplantations of PBS displayed a similar reduction in saliva production, to 51% ± 5% at 3 months post-irradiation (Supplementary Information Fig. S7A). Primary human salispheres were isolated and transplanted 2–5 days following isolation. Saliva flow in mice transplanted with 100,000 human salisphere cells increased significantly to 79% ± 8% ($p < .001$) and 70% ± 7% ($p < .05$) of pre-irradiation saliva flow at 2 and 3 month human salisphere post-irradiation, respectively (Fig. 4A). Area under curve analysis demonstrated a significant ($p < .01$) increase in saliva production in human salisphere transplanted mice, compared to irradiated controls (Fig. 4B). Increasing the number of transplanted cells led to an increase in gland functionality, emphasizing the cell dose- dependent nature of the hyposalivation rescue (Fig. 4C). The range of functional responses to human salisphere transplantation can be partly explained by the heterogeneous nature of human biopsy material, as transplants from some donors were more efficacious than others (Supplementary Information Fig. S7B). Transplantation of human salisphere cells also increased the wet weight ($p < .05$) of transplanted glands in a time-dependent manner when compared to time-matched irradiated controls and sham transplanted animals (Fig. 4D).

To examine the effect of human salisphere cell therapy on the regenerative potential of SGs, we assessed the possibility of irradiated and transplanted glands to generate new primary salispheres in culture. Irradiation alone reduced salisphere formation to 33% ± 7% SEM of age-matched non-irradiated controls (Fig. 4E, “0” group), reflecting a deficit in resident SG stem/progenitor cells. Two months after irradiation, animals receiving 100,000 cells demonstrated enhanced salisphere formation compared to cultures generated from the irradiated control group (Fig. 4E). This effect was further dependent on transplanted cell dose, as mice receiving 1,000 or 10,000 cells showed less salisphere generation capability (Fig. 4E). Salisphere cultures from transplanted glands could furthermore be maintained in vitro in 3D cultures for more passages, producing more salispheres than non-transplanted glands, indicating a higher proliferative potential (Fig. 4F). These data provide further evidence that human salisphere transplants replenish SG stem/progenitor cell populations.

Previous reports from our lab and others have suggested that stem and progenitor populations reside within salisphere cultures from rodent SGs, however this remains unresolved in human salisphere cultures (Lombaert et al., 2008a; Nanduri et al., 2011; Pringle et al., 2013). In order to assess the potential of stem/progenitor cell populations within the human salisphere pool, we selected cells expressing the established stem cell marker protein c-Kit, from human salisphere cultures. c-Kit^{+} cell derived salipsheres were indeed capable of organoid differentiation in vitro and also rescued saliva production in vivo, with a much lower cell number than their unfractionated counterparts (Fig. 5A, 5B) or c-Kit^{-} cells (data not shown). Our recent study using autologous C57BL/6

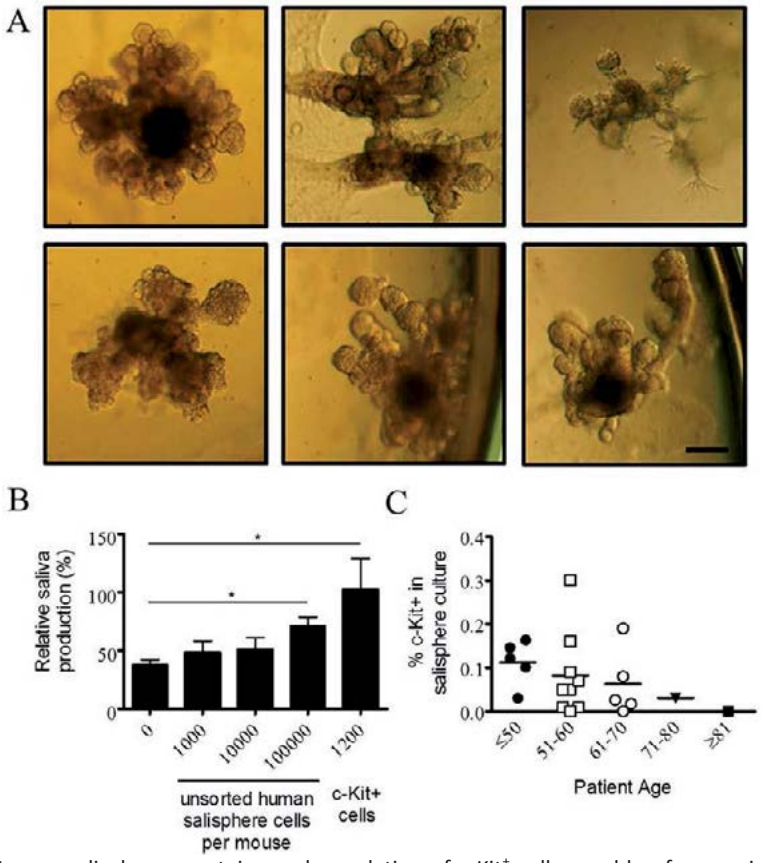

Figure 5. Human salispheres contain a subpopulation of c-Kit$^+$ cells capable of organoid formation and functional rescue. **(A)**: Single c- Kit$^+$ cell derived organoids cultured for 10 days. Scale bar = 50 µm. **(B)**: Relative saliva production in mice receiving 100, 1,000, or 100,000 unselected human salisphere cells total, no cell transplant ("0" group), or 600 c-Kit$^+$ cells per gland. Scale bars = SEM. n≥7 mice per group. *, p<.05, Student's t test. Data are normalized to pre-irradiation saliva production value for each animal. **(C)**: Frequency of c-Kit$^+$ cells in patient biopsies grouped by age.

unselected salisphere- derived cells for transplantation demonstrated a 10% increase in function of the recipient SG at 3 months post-transplantation (Nanduri et al., 2014). Here, we demonstrate improvement in SG function of 33.30% and 64.20% following transplantation of unselected and c-Kit$^+$ human salisphere cells respectively, at 2 months following transplantation. Acknowledging caveats of the different mouse models used, these data suggest firstly that human salisphere cells hold great therapeutic promise for rescue of hyposalivation and secondly that purification of a potent stem cell subset from the heterogeneous salisphere population may enhance hyposalivation recovery. It should be noted, however, that the frequency of c-Kit$^+$ cells in primary cultures is extremely low, and appears even to decrease with age, in agreement with our previous studies showing decrease in

overall primary salisphere yield with age (Feng et al., 2009; Maimets et al., 2015). These data suggest that other, more abundant stem cell marker proteins may be more suitable (Fig. 5C).

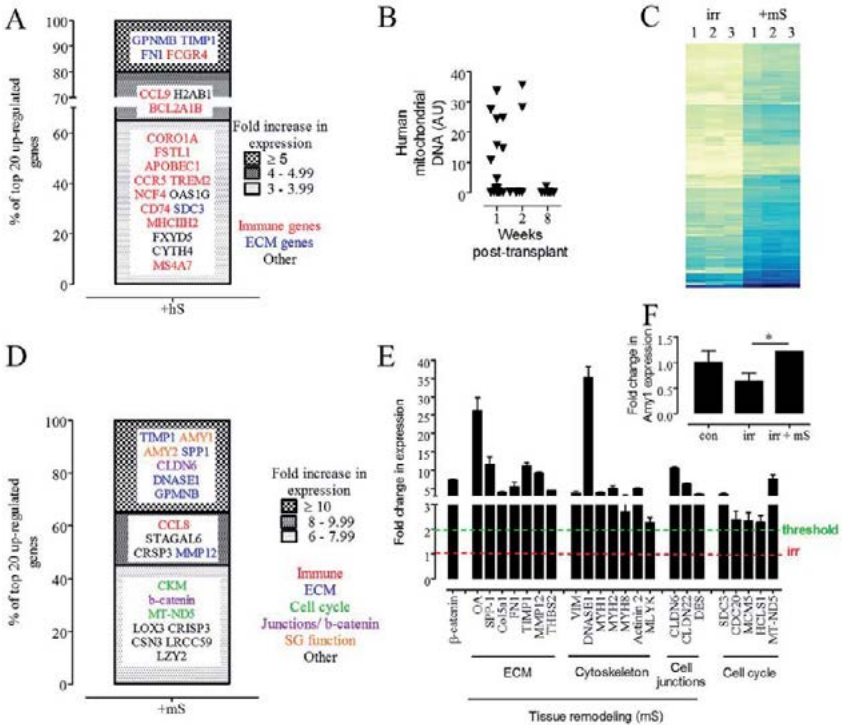

Figure 6. Gene expression profiles of SGs 1 week following human and murine salisphere transplantation. **(A)**: Top 20 upregulated genes in human salisphere (hS)-transplanted glands, following whole genome microarray analysis and compared with irradiated control mice. "Upregulated" defined as significantly different expression of a gene ($p < .05$) from irradiated control group, with a minimal fold increase in expression of 2. **(B)**: Detection of human mitochondrial DNA in hS-transplanted SGs by quantitative polymerase chain reac- tion. Each data point represents a separate mouse; all mice received 100,000 hS cells. **(C)**: Heat map showing differential expression of genes in NSG mice transplanted with autologous NSG salispheres (irr+mS), compared to irradiated (irr) NSG controls. Numbers represent biological replicates. **(D)**: Top 20 upregulated genes in mS-transplanted glands following whole genome microarray analysis and compared with irradiated control mice. "Upregulated" defined as (B). **(E)**: Functional grouping of upregulated genes from mS-transplanted glands. Grouping was performed using EnrichR software, grouping genes into functional related clusters. Gene acronyms are standard Gene Symbol abbreviations. All data are relative to irradiated control expression (irr) and above a fold increase of 2 (threshold). n=3 biological replicates in transplanted and control group, errors bars = SEM. **(F)**: Expression of SG-associated α-amylase in NSG control (con), 5 Gy-irradiated and salisphere-transplanted (irr+mS), and time-matched irradiated NSG glands (irr). n=3 biological replicates, Student's t test, *, $p < .05$. Error bars = SEM. Abbreviations: ECM, extracellular matrix; SG, salivary gland.

To investigate to what extent the observed functional recovery was dependent on the continued presence of the human salisphere-derived cells, human chimerism was assessed using qPCR and

primers specific for human mitochondrial DNA (for assay design see Supplementary Information Fig. S8). Human cells were detected at up to 9% ± 3% SEM of total cells following transplantation, a frequency which suggests the functional rescue observed might not completely be attributed to human cell engraftment. Regenerative signals emanating from the endogenous murine cells following human salisphere transplantation might also contribute to rescue. Analysis of RNA extracted from human salisphere- transplanted SGs 1 week post-transplantation, when human cells were most easily detected, revealed 471 probes upregulated, in comparison to time-matched irradiated control SGs (GEO accession number: GSE72871). The predominant function of these genes however appeared to be immune rejection/reaction (Fig. 6A; Supplementary Information Fig. S9A). Apparently, NSG mice still exhibit an immune response, which may explain spread in engraftment observed and the reduction in human cells present in the recipient tissue over time (Fig. 6B). Whole genome mRNA expression analysis of syngeneic salisphere transplantation (NSG salispheres into NSG SGs) was performed to circumvent the immune rejection phenotype, and revealed significant ($p < .05$) upregulation of 510 genes at 1 week following salisphere transplantation compared to irradiated controls (Fig. 6C, 6D) (GEO accession number: GSE72871). Using a significance threshold of $p < .05$ and a minimal fold increase of 2, upregulated genes could be functionally organized into tissue remodeling (including extracellular matrix (ECM)-, cytoskeletal- and cell junction-associated genes) and proliferation-associated genes, in addition to highly upregulated expression of the canonical Wnt-signaling regulator β-catenin (Fig. 6E). Further analysis demonstrated a moderate upregulation of soluble factors associated with SG branching and development (transforming growth factor (TGF)b1, TGFb3, bone morphogenetic protein1) (Han et al., 2013; Maimets et al., 2015), SG stem cell maintenance (insulin growth factor, EGF) (Supplementary Information Fig. S9B), and SG functionality (α-amylase, AQP-1, DCPP2, DCPP3, PSP) (Fig. 6F; Supplementary Information Fig. S9C). In order to translate these data to xeno-transplants of human salisphere cells, we returned to check the expression of genes identified in Figure 6C–6E in NSG glands transplanted with human salisphere cells. Indeed, murine-specific transcripts upregulated in syngeneic salisphere microarray analysis, including regulators of the Wnt pathway, were also upregulated in the human salisphere xenotransplantation microarray (Fig. 7A, 7B). To assess the expression of some of the translated proteins, we performed immunohistochemical and histological stainings on human salisphere-transplanted NSG SGs. We observed β-catenin expression, the key mediator of the canonical Wnt-signaling pathway, in the ducts of human salisphere transplanted glands, whereas it was lost in irradiated but non-transplanted glands (Fig. 7C). Similarly, immunostainings for collagen (Fig. 7D) and fibronectin (Fig. 7E) validated the microarray data suggesting upregulation of extracellular matrix proteins, and Ki67 labeling further confirmed the presence of more proliferating cells in both ducts and acinar cell compartments of human salisphere-transplanted glands (Fig. 7F; Supplementary infor-

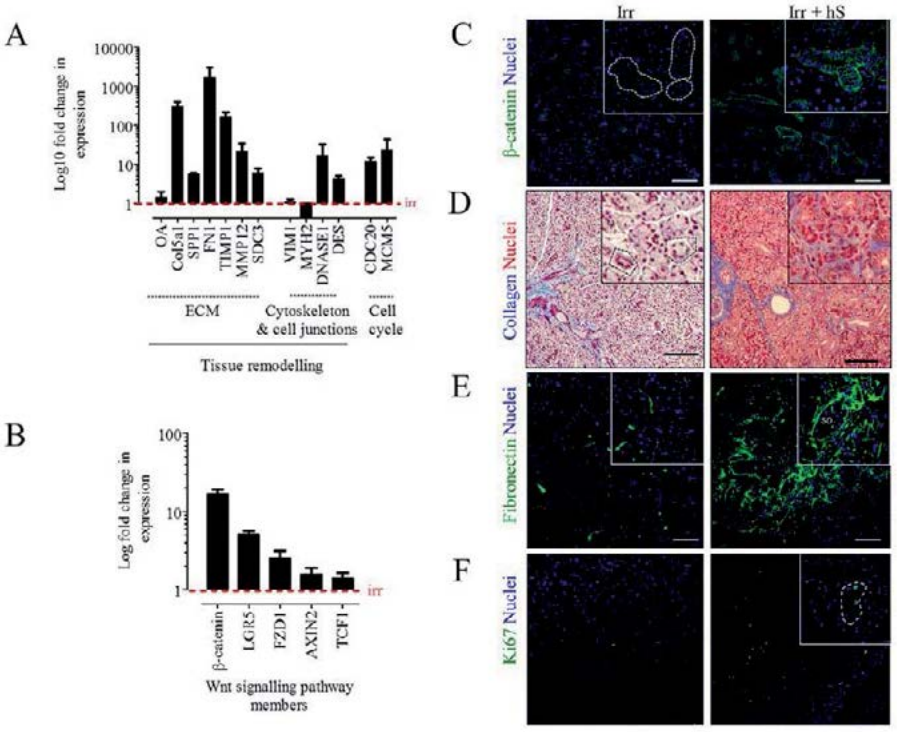

Figure 7. Gene and protein expression profiles of SGs transplanted with human salisphere-derived cells. **(A)**: Expression of ECM, cytoskeletal, and cell proliferation-associated genes upregulated in autologous salisphere microarray analysis. All data are relative to irradiated control expression (irr). n=≥3 biological replicates. Gene acronyms are standard Gene Symbol abbreviations. Error bars = SEM. **(B)**: Relative expression of canonical Wnt-signaling mediators in human salisphere transplanted glands. All data are relative to irradiated control expression (irr). n=4 biological replicates. Error bars = SEM. **(C–F)**: Stainings for β-catenin (C), Masson's Trichrome staining for collagen (D), fibronectin (E), and Ki67 (F). Nuclear counterstainings are DRAQ5 for fluorescent images or hematoxylin for bright field microscopy. Scale bars = 100 µm. Inset boxes represent high resolution of inset boxes in left columns. Abbreviations: SD, striated duct; ECM, extracellular matrix; irr, time-matched irradiated control; irr+hS, 1 week following human salisphere transplantation.

mation Fig. S9A, S9B). Interestingly, when c-Kit$^+$ cells were transplanted and mice sacrificed at the same time point (1 week following transplantation), increased expression of some genes in this regeneration-associated cohort, including the Wnt signaling reporter Axin-2 was observed (Supplementary Information Fig. S11A, S11B). This suggests that a small number of selected c-Kit$^+$ stem/progenitor cells have similar potencies as unselected human salisphere cells, with respect to initiating functional recovery of the gland. The enhanced expression of these genes in recipient SGs at 1 week after c-Kit$^+$ salisphere cell transplantation and the greater rescue in SG function at 2 months following transplant, compared to unselected cells (Supplementary Information Fig. S11C)

would suggest indeed that subsets of human salisphere cells such as c-Kit$^+$ cells are superior in inducing regeneration than others.

These combined data suggest that transplanted human salisphere-derived cells restore homeostasis of the SGs by a combination of engraftment, proliferation, differentiation, and potential stimulation of recipient cells and that salispheres contain subsets of cells with greater regenerative potential.

DISCUSSION

Adult stem cells hold great therapeutic promise in regenerative medicine, however, translation to the clinic is hampered by rarity of data showing engraftment and functional capabilities of these cells. Here, we characterize for the first time the proliferation, differentiation, and regenerative potential of stem/progenitors from the human SG, at the single cell level in vitro, including their long-term engraftment capabilities in vivo. We additionally demonstrate that a population of more potent stem cells, namely c-Kit$^+$ cells, exists within the human SG stem cell pool. These cells, capable of rescuing hyposalivation after low cell dose transplantation, are the first documentation of in vivo functional properties of a defined stem cell population from the adult human SG. Our results follow on recent studies in the murine SG, where c-Kit$^+$, CD24$^+$ CD29$^+$, or CD24$^+$c-Kit$^+$Sca-1$^+$ cells rescued function of the irradiated SG and differentiated and engrafted within the recipient mouse (Lombaert et al., 2008a; Nanduri et al., 2014; Xiao et al., 2014). Of note, 300 transplanted c- Kit$^+$ murine SG stem cells per SG were capable of rescuing hyposalivation in vivo, comparable with 500 human c-Kit$^+$ SG cells per SG (Lombaert et al., 2008a). Indeed, we have previously shown the expression of a panel of stem cell associated marker proteins in human salispheres, suggesting that defining the specific stem cell may permit even greater therapeutic potential for the treatment of hyposalivation (Pringle et al., 2013). While many stem cell populations have been characterized in mouse tissues and some have been tested in human stem cell populations, few human stem cell populations have shown engraftment and functional rescue potential such as that presented in this study (Han et al., 2013; Huch et al., 2013; Ng et al., 2014; Notta et al., 2011; Schuijers and Clevers, 2012; Shackleton et al., 2006; Yui et al., 2012).

Further to these data, we also suggest that transplantation of human salisphere cells and consequential regeneration might involve stem cell-associated signals for the recipient SG. Our expression analysis revealed enhancement of ECM protein expression and stimulation of endogenous stem cell proliferation as probable mediators of this effect. Several studies suggest that murine SG stem cells are receptive to such signaling from TGF/ BMP, FGF, and Wnt signaling

pathways (Haara et al., 2011; Hai et al., 2012; Hoffman et al., 2002; Jaskoll et al., 2005; Jaskoll and Melnick, 1999; Lombaert et al., 2006; Maimets et al., 2016). The low radiation dose (5 Gy) used to induce SG hypofunction in this study (chosen because of the severity of esophageal tract side effects in NSG mice irradiated with higher doses) permits the survival of endogenous murine SG stem/progenitor cells with regenerative potential, which might be amenable to signaling stimuli from transplanted human salisphere cells. Indeed, the study by Hai et al. demonstrated recovery of the post-irradiation murine SG following transient Wnt pathway activation (and not following irradiation alone), lending further weight to our hypothesis that Wnt signaling plays a critical role in functional recovery of radiation-damaged SG (Hai et al., 2012).

We present the first evidence showing therapeutic potential of a new population of clinically relevant adult human stem cells. Syngeneic transplantation studies in the mouse have demonstrated long-term engraftment potential of salisphere cells, and we predict great engraftment potential of human salisphere cells, and amelioration of xerostomia, when autologous transplantations are performed. The autologous setting may provide better incorporation of the transplanted cells in SGs in patients in which few or no resident stem cells survive (Lombaert et al., 2008a; Nanduri et al., 2014; Xiao et al., 2014). Surviving endogenous patient cells might additionally benefit from stimulation via transplanted salisphere cells and provide a boost to SG function (Lombaert et al., 2008b).

CONCLUSION

In summary, we showed the presence of SG stem/progenitor cells in cultured human salispheres. These cells are capable of self-renewal and differentiation, which when transplanted into irradiated recipients, restore glandular function. The present data highlight the promising therapeutic potential of human SG stem/progenitor-like cells cultured from biopsy material for treatment of radiation-induced hyposalivation.

Author Contributions

S.P.: conception and design, collection and/or assembly of data, data analysis and/or interpretation, and manuscript writing; M.M., M.v.d.Z., and D.v.G.: collection and/or assembly of data and data analysis and/or interpretation; M.A.S.: conception and design and provision of study materials or patients; E.Z.: data analysis of interpretation; M.J.H.W.: conception and design and provision of study materials or patients; G.d.H. and R.v.O.: conception and design and manuscript writing. R.P.C. conception and design, data interpretation, financial support, and manuscript writing.

Disclosure of Potential Conflicts of Interests

The authors indicate no potential conflicts of interests.

SUPPORTING INFORMATION

Supplementary Methods

PI Cell Cycle Analysis

Human salispheres at passages 1 and 5 cultured as above were harvested and processed to single cells from self-renewal gels, as described above for passaging. After washing in PBS, cells were fixed in 1mL 70 % ethanol, added drop-wise to the pellet, and incubated on ice for 30 minutes. Cells were collected by centrifugation washed twice with PBS and treated with Ribonuclease A, to remove residual RNA (50uL of 100 µg/mL in PBS RNAse stock solution per sample (Sigma Aldrich). 400 µL of PI solution (50 µg/mL in PBS) was added to each sample, and incubated at room temperature for 5-10 minutes before analysis using the BD FACSAria LSR-II Flow Cytometer and FACSDiva software.

Karyotype Spread Analysis

Primary human salisphere cultures were generated and 20 hours prior to harvesting, medium was supplemented with colcemid (Gibco) at 12.5 ng/mL. Chromosome preparations of cells were made after short-term culture, using standard cytogenetic techniques. The chromosomes were G-banded using pancreatin and karyotypes expressed in accordance with the ISCN 2013.

Alcian Blue Staining

8 µm sections of primary salispheres were incubated with 1 % alcian blue (Chroma-Gesellschaft) in 3 % acetic acid pH 2.5 (30 min, RT). Slides were then washed in water, counterstained with 0.1 % neutral fast red (Fisher Scientific) containing 2.5 % aluminum sulphate and washed again and dehydrated and mounted as standard.

PCR

Total RNA was extracted from primary salisphere cultures or whole human submandibular salivary gland using the Absolutely RNA Miniprep kit (Agilent Technologies), including DNase incubation, as per manufacturer's instructions. One µg of total RNA was reverse transcribed using 0.5 µg oligo$(dT)_{15-18}$ primers, 0.5 mM dNTPs, 1X First-strand Buffer, 0.01M DTT, 400 U RnaseOut and 200 U of M-MLV Reverse Transcriptase (all Invitrogen), in a total volume of 20 µL per reaction. One hundred ng of resultant cDNA was mixed with PCR buffer, 0.2mM dNTPs , 1.5 mM $MgCl_2$, 50 U Taq polymerase (all Invitrogen) and 2 µM of both forward and reverse primers for genes of interest, to a total volume of

50 µL in deionized water. Samples were subjected to a 3-step PCR reaction, using the PTC-100 Peltier Thermal cycler (MJ Research) and PCR products separated by gel electrophoresis using 2 % agarose-TAE gels containing ethidium bromide and visualized by UV illumination. Primer sequences can be found in Table S1.

Supplementary Figures

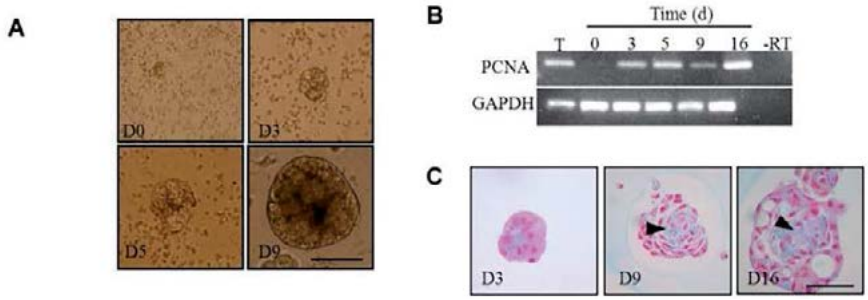

Figure S1 *Human salisphere cells increase in size in culture, are proliferative and are capable of spontaneous differentiation*. (A) Representative phase contrast microscopy of primary human salispheres at indicated days in culture. (B) Time course analysis of proliferating cell nuclear antigen (PCNA) expression in human salisphere culture. GAPDH = glyderaldehyde-3-phosphate dehydrogenase internal control gene; T = SG tissue control; -RT = control reaction without reverse transcriptase enzyme. (C) Detection of mucins (blue) using Alcian Blue staining, in human salispheres at indicated days in primary salisphere culture. Arrows denote mucin-producing areas. Nuclei counterstained with Neutral Fast Red. Scale bars represent 50 µm.

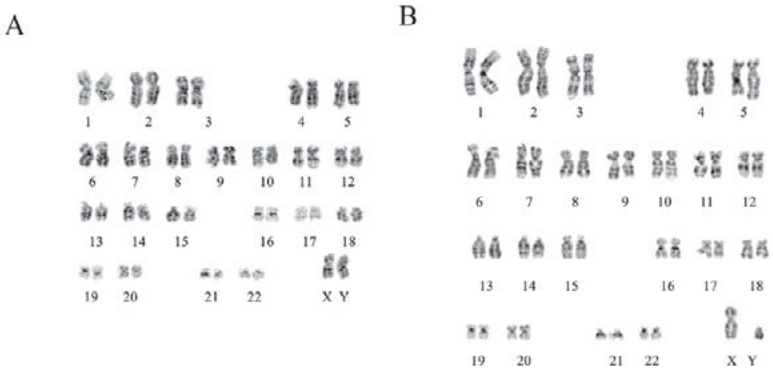

Figure S2 *Primary salisphere cultures do not harbor karyotypic abnormalities.* Representative karyotype spread analyses of primary salispheres generated from female (A) and male (B) patient biopsy material.

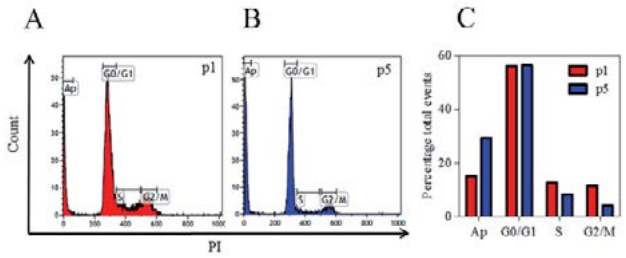

Figure S3 *Human salispheres undergo apoptosis and differentiation at later passages in self-renewal assay*. Representative cell cycle analysis plots of human salispheres analyzed at passage 1 (A) and 5 (B). Proportion of apoptotic (Ap), cells in G0/G1 (quiescent), Synthesis phase (S) and G2/mitotic (G2/M) cells are represented in C, where more apoptotic and less mitotic cells are noted in cells from later passage cultures. *n* = 1.

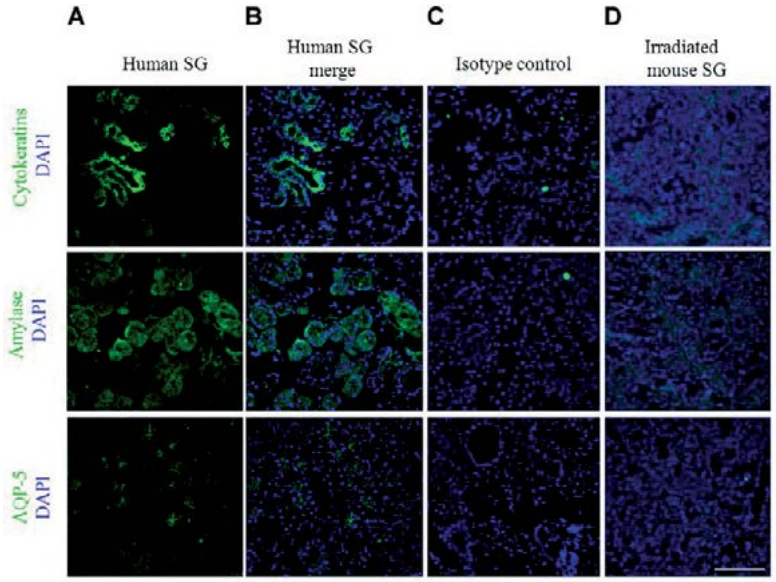

Figure S4 *Anti- Cyt, α-amylase and AQP-5 antibodies detect human proteins, with minimal cross-reactivity in the irradiated mouse salivary gland*. (A and B) Positive control immunostainings from frozen human salivary gland sections. Single fluorescence channel and merges are shown. (C) Isotype controls using human salivary gland tissue. (D) Irradiated mouse salivary gland exposed to the same labeling protocol. Nuclei are counterstained with DAPI. Scale bar represents 100 µm

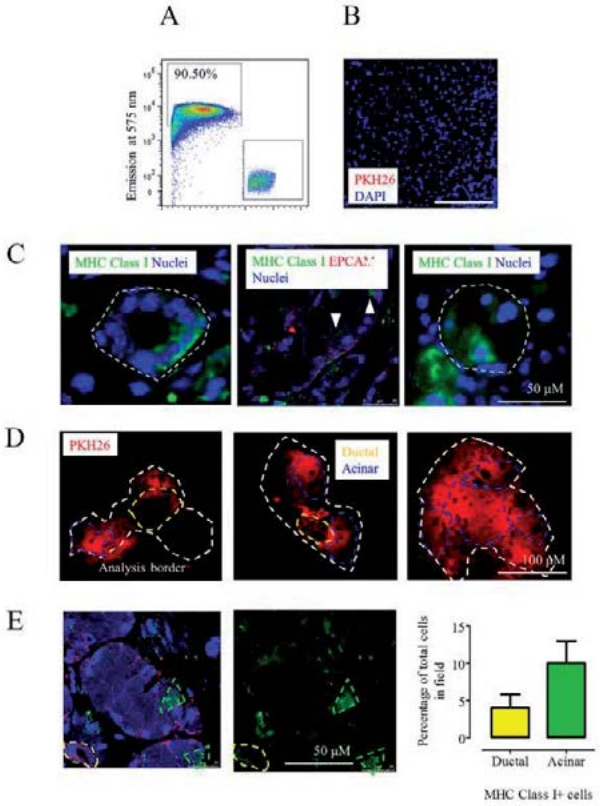

Figure S5 *Dynamics of transplanted human salisphere cells following submandibular SG transplantation.* A) PKH26-labelling of hS cells detected by fluorescence emission at 575nM and plotted against forward scatter. Inset = unstained control. B) Volume of PKH26 staining buffer equivalent to that used for hS cell transplantation underwent all steps in the staining protocol, in the absence of any cells (dye control solution). Dye control solution was injected as per SG transplantations, and animal was sacrificed 60 days post-transplantation. Nuclei counterstained with DAPI. Scale bar = 500 µM. C) Transplanted human cells detected using human specific anti major histocompatibility complex class I (MHC Class I) antibody show ductal (white outline; first panel), and both mucous (white arrows; second panel) and serous acinar cells (white outline; last panel) morphology. An antibody highlighting all epithelial cells, including acinar cells, was used for definition in the middle panel. D) Examples of quantification of ductal- and acinar-like cells in PKH26+ foci. E) Examples of quantification of ductal- and acinar-like MHC Class I-positive transplanted human salisphere cells. C) – E) scale bars as indicated.

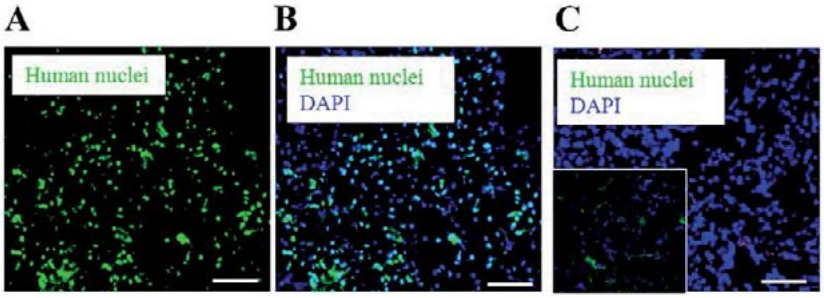

Figure S6 *Anti-human nuclei antibody detects nuclei in human salivary gland and not in irradiated mouse salivary gland.* (A and B) Human salivary gland tissue immunostained using anti-human nuclei antibody, showing approximately 50 % immunopositivity. Single channel and merged fluorescence images are shown. (C) Isotype control reaction did not demonstrate any immunoreactivity, and irradiated mouse salivary gland tissue demonstrated only non-specific staining typical of irradiated salivary tissue, when fluorescence was greatly enhanced (C inset). Scale bars 100 µm.

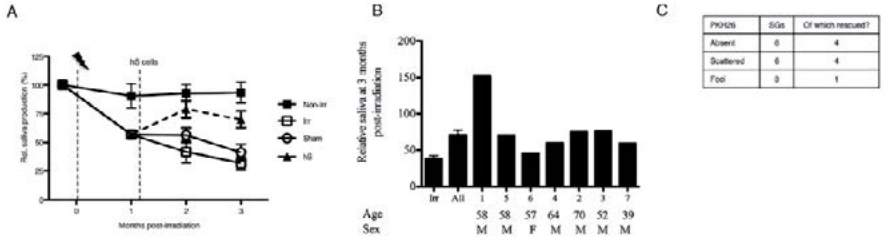

PKH26	SGs	Of which rescued?
Absent	6	4
Scattered	6	4
Foci	3	1

Figure S7 *Sham transplants do not result in functional recovery, and heterogeny of response to human salisphere transplantation is partially due to patient variability.* (A) 3 mice were injected with transplantation medium only, in equivalent volumes to human salisphere transplants, and followed over time. Bars = S.E.M. Remaining data points are same as those presented in Fig 4a. (B) Breakdown of functional recovery data by donor. Error bars represent mean and S.E.M. 'All' groups represent mean saliva production from 7 individual patients detailed. Irr = irradiated control mouse, n = 10. M = male; F = female. (C) Morphologies of PKH26 observed in transplanted glands 2-3 months following transplantation, and proportion of which demonstrating functional rescue of saliva production. Table is adapted from that in Figure 2.

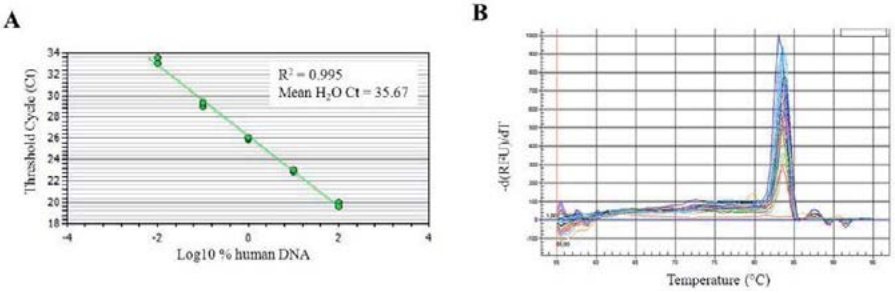

Figure S8 *Primers specific for human mitochondria can be used determine proportion of human cells in a sample.* (A) The threshold cycle of product amplification from ten-fold dilutions of human DNA were used to create a standard curve from which to analyze unknown samples. (B) Melt curve analysis to show purity of amplicon produced by anti-human mitochondrial primer pair.

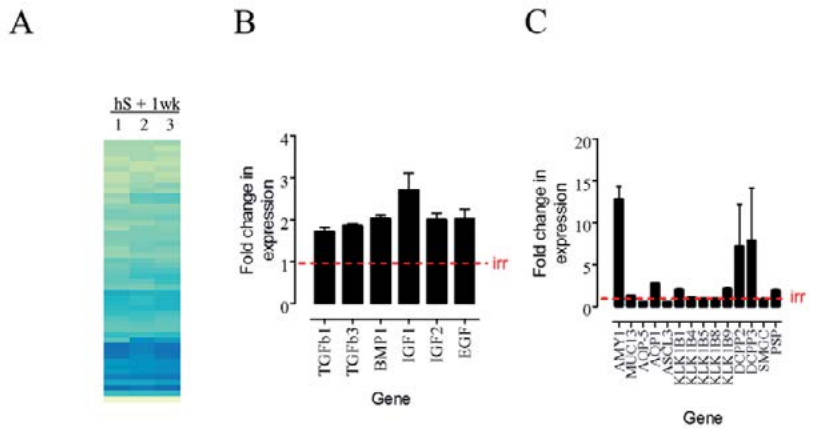

Figure S9 *Human salisphere stimulates expression of soluble mediators of SG development, and expression of some SG functional genes.* A) Heatmap depicting probes significantly upregulated genes in 3 irradiated NSG submandibular SGs following transplantation with human salisphere cells, in comparison to irradiation alone. Numbers refer to individual mice. B) Mean fold change in soluble mediator expression following autologous salisphere transplantation. C) Mean fold change in expression of genes associated with SG function, following autologous salisphere cell transplantation. In B-C) data are expressed 1 week following transplantation, relative to expression in time-matched irradiated controls. *n* = 3 biological replicates.

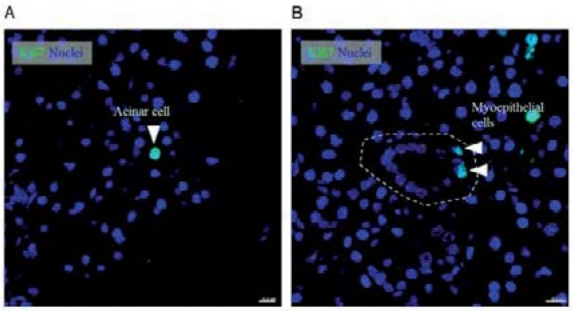

Figure S10 *Sup*
plementary irradiated or hS-transplanted tissue immunostainings. (A) Ki67 expression in acinar (A) and myoepithelial cells (B) following human salisphere transplantation. Scale bar = 10 µm. Nuclei counterstained with DRAQ5.

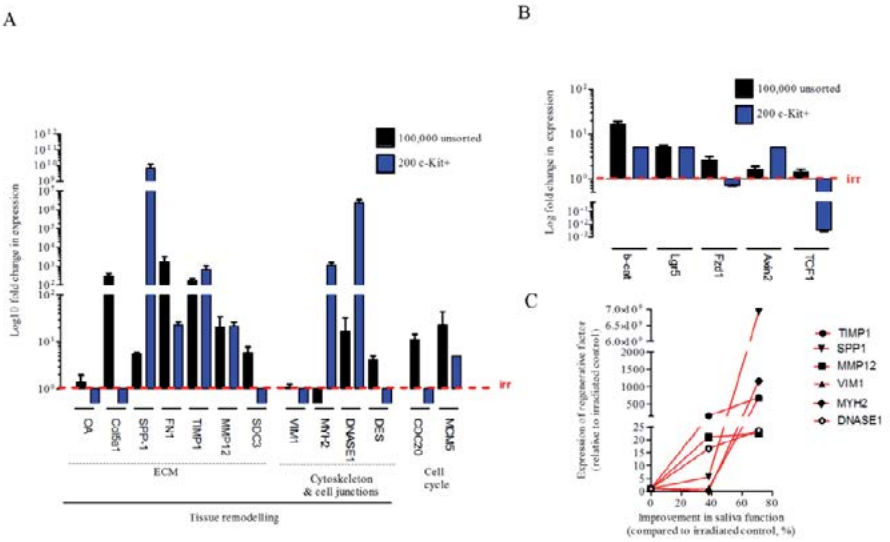

Figure S11 *c-Kit+ cells induce higher expression of regeneration-associated genes than unselected human salisphere cells, but do not induce Wnt signaling.* (A) Expression of identified gene cohort from Figure 7, following transplantation with 200 c-Kit+ cells per mouse, compared to 100,000 unselected human salisphere cells. Mice were sacrificed 1 week post-transplantation, as in Figure 7. (B) Expression of members of Wnt signaling pathway, previously demonstrated as upregulated after unselected human salisphere transplantation, when transplanted with 200 c-Kit+ cells. c-Kit+ cells from 3 separate patient isolations were transplanted. Data in (A) and (B) represents expression normalized to that in irradiated (non-transplanted) glands (**irr**; red line). C) Highest expression of some paracrine signaling genes at 1 week following transplantation was correlated with highest functional recovery (c-Kit+ cell transplantation –versus- unselected cell transplantation) of the salivary gland at 2 months following transplantation. n = ≥ 3 transplantations from separate patient isolations for gene expression data, and ≥6 for saliva functional data.

Supplementary Table

Gene	Gene Symbol	Species (m/h)	Forward primer 5'-3'	Reverse primer 5'-3'
Proliferating cell nuclear antigen	PCNA	h	ggctctagcctgacaaatgc	gcctccaacaccttcttgag
Glyceraldehyde-3-dehydrogenase	GAPDH	h	agcagttggtggtgcaggag	tggagtccactggcgtcttc
Mitochondrial DNA	-	h	tacgagtacaccgactacgg	ttagacgtccgggaattg
Fibronectin	FN1	m	gcgactctgactggccttac	ccgtgtaagggtcaaagcat
Vimentin	VIM	m	atgcttctctggcacgtctt	agccacgctttcatactgct
Claudin6	CLDN6	m	tgagtccaagctccacctct	gaactcttgggactgggaca
Cell division cell protein 20	CDC20	m	agaccacccctagcaaacct	gagaccaggctttctgatgc
Syndecan 3	SDC3	m	agctgcagtcttggggacta	acccactgcctcttctctca
Secreted phosphoprotein 1	SPP1	m	tgcacccagatcctatagcc	ctccatcgtcatcatcatcg
Glyceraldehyde-3-dehydrogenase	GAPDH	m	tgcaccaccaactgcttagc	ggcatggactgtggtcatgag
Osteoactivin	GPNMB	m	aaggggtatgctgtccctct	ctgcagcaacctgaaatcaa
b-catenin	CTNNB	m	atggagccggacagaaaagc	cttgccactcagggaagga
DNASE1	DNASE1	m	actcaatcgggacaaacctg	atttccacagggttcacagc
Tissue inhibitor of metalloproteinases 1	TIMP1	m	attcaaggctgtgggaaatg	ctcagagtacgccagggaac
Minichromosome maintenance complex component 5	MCM5	m	gaggaccaggagatgctgag	ttgaggcgatagagcacctt
Type 5 Collagen a1	COL5A1	m	ggtccctgacacacctcagt	tgctcctcaggaacctctgt
Desmin	DES	m	gtgaagatggccttggatgt	gtagcctcgctgacaacctc
Myosin heavy chain 1	MYH1	m	cttcaaccaccacatgttcg	aggtttgggcttttggaagt
Myosin heavy chain 2	MYH2	m	ggccaaaatcaaagaggtga	cgtgcttctccttctcaacc
Myosin heavy chain 8	MYH8	m	tacaggcgaaggtgaaatcc	cctcctgtgctttccttcag
Matrix metalloprotease 12	MMP12	m	tttcttccatatggccaagc	ggtcaaagacagctgcatca
Tyrosine 3-monooxygenase/tryptophan 5-monooxygenase activation protein	YWHAZ	m	ttacttggccgaggttgct	tgctgtgactggtccacaat
Frizzled 1	FZD1	m	caaggtttacgggctcatgt	gtaacagccggacaggaaaa
T-Cell Factor	TCF1	m	ggcctcctcttcccagtaac	ggagcagcagtgtcaatgaa
Axis inhibition protein 2	AXIN2	m	gggggaaaacacagcttaca	ttgactgggtcgcttctctt
Leucine rich repeat containing G-protein coupled receptor 5	LGR5	m	accagcttaccccatgactg	ctcctgctctaaggcaccac

Table S1. Primer sequences

REFERENCES

Baglioni, S., Francalanci, M., Squecco, R., Lombardi, A., Cantini, G., Angeli, R., Gelmini, S., Guasti, D., Benvenuti, S., Annunziato, F*., et al.* (2009). Characterization of human adult stem-cell populations isolated from visceral and subcutaneous adipose tissue. FASEB J *23*, 3494-3505.

Banh, A., Xiao, N., Cao, H., Chen, C.H., Kuo, P., Krakow, T., Bavan, B., Khong, B., Yao, M., Ha, C*., et al.* (2011). A novel aldehyde dehydrogenase-3 activator leads to adult salivary stem cell enrichment in vivo. Clin Cancer Res *17*, 7265-7272.

Burlage, F.R., Coppes, R.P., Meertens, H., Stokman, M.A., and Vissink, A. (2001). Parotid and submandibular/sublingual salivary flow during high dose radiotherapy. Radiother Oncol *61*, 271-274.

Cotroneo, E., Proctor, G.B., and Carpenter, G.H. (2010). Regeneration of acinar cells following ligation of rat submandibular gland retraces the embryonic-perinatal pathway of cytodifferentiation. Differentiation *79*, 120-130.

Cotroneo, E., Proctor, G.B., Paterson, K.L., and Carpenter, G.H. (2008). Early markers of regeneration following ductal ligation in rat submandibular gland. Cell Tissue Res *332*, 227-235.

David, R., Shai, E., Aframian, D.J., and Palmon, A. (2008). Isolation and cultivation of integrin alpha(6)beta(1)-expressing salivary gland graft cells: a model for use with an artificial salivary gland. Tissue Eng Part A *14*, 331-337.

Denny, P.C., Chai, Y., Klauser, D.K., and Denny, P.A. (1993). Parenchymal cell proliferation and mechanisms for maintenance of granular duct and acinar cell populations in adult male mouse submandibular gland. Anat Rec *235*, 475-485.

Feng, J., van der Zwaag, M., Stokman, M.A., van Os, R., and Coppes, R.P. (2009). Isolation and characterization of human salivary gland cells for stem cell transplantation to reduce radiation-induced hyposalivation. Radiother Oncol *92*, 466-471.

Haara, O., Fujimori, S., Schmidt-Ullrich, R., Hartmann, C., Thesleff, I., and Mikkola, M.L. (2011). Ectodysplasin and Wnt pathways are required for salivary gland branching morphogenesis. Development *138*, 2681-2691.

Hai, B., Yang, Z., Shangguan, L., Zhao, Y., Boyer, A., and Liu, F. (2012). Concurrent transient activation of Wnt/beta-catenin pathway prevents radiation damage to salivary glands. Int J Radiat Oncol Biol Phys *83*, e109-116.

Han, X., Chen, M., Wang, F., Windrem, M., Wang, S., Shanz, S., Xu, Q., Oberheim, N.A., Bekar, L., Betstadt, S*., et al.* (2013). Forebrain engraftment by human glial progenitor cells enhances synaptic plasticity and learning in adult mice. Cell Stem Cell *12*, 342-353.

Hoffman, M.P., Kidder, B.L., Steinberg, Z.L., Lakhani, S., Ho, S., Kleinman, H.K., and Larsen, M. (2002). Gene expression profiles of mouse submandibular gland development: FGFR1 regulates branching morphogenesis in vitro through BMP- and FGF-dependent mechanisms. Development *129*, 5767-5778.

Huch, M., Dorrell, C., Boj, S.F., van Es, J.H., Li, V.S., van de Wetering, M., Sato, T., Hamer, K., Sasaki, N., Finegold, M.J*., et al.* (2013). In vitro expansion of single Lgr5+ liver stem cells induced by Wnt-driven regeneration. Nature *494*, 247-250.

Jaskoll, T., Abichaker, G., Witcher, D., Sala, F.G., Bellusci, S., Hajihosseini, M.K., and Melnick, M. (2005). FGF10/FGFR2b signaling plays essential roles during in vivo embryonic submandibular salivary gland morphogenesis. BMC Dev Biol *5*, 11.

Jaskoll, T., and Melnick, M. (1999). Submandibular gland morphogenesis: stage-specific expression of TGF-alpha/EGF, IGF, TGF-beta, TNF, and IL-6 signal transduction in normal embryonic mice and the phenotypic effects of TGF-beta2, TGF-beta3, and EGF-r null mutations. Anat Rec *256*, 252-268.

Jones, P.H., and Watt, F.M. (1993). Separation of human epidermal stem cells from transit amplifying cells on the basis of differences in integrin function and expression. Cell *73*, 713-724.

Kajstura, J., Rota, M., Hall, S.R., Hosoda, T., D'Amario, D., Sanada, F., Zheng, H., Ogorek, B., Rondon-Clavo, C., Ferreira-Martins, J*., et al.* (2011). Evidence for human lung stem cells. N Engl J Med *364*, 1795-1806.

Katsumata, O., Sato, Y., Sakai, Y., and Yamashina, S. (2009). Intercalated duct cells in the rat parotid gland may behave as tissue stem cells. Anat Sci Int *84*, 148-154.

Kaukua, N., Shahidi, M.K., Konstantinidou, C., Dyachuk, V., Kaucka, M., Furlan, A., An, Z., Wang, L., Hultman, I., Ahrlund-Richter, L*., et al.* (2014). Glial origin of mesenchymal stem cells in a tooth model system. Nature *513*, 551-554.

Kishi, T., Takao, T., Fujita, K., and Taniguchi, H. (2006). Clonal proliferation of multipotent stem/progenitor cells in the neonatal and adult salivary glands. Biochem Biophys Res Commun *340*, 544-552.

Knox, S.M., Lombaert, I.M., Haddox, C.L., Abrams, S.R., Cotrim, A., Wilson, A.J., and Hoffman, M.P. (2013). Parasympathetic stimulation improves epithelial organ regeneration. Nat Commun *4*, 1494.

Knox, S.M., Lombaert, I.M., Reed, X., Vitale-Cross, L., Gutkind, J.S., and Hoffman, M.P. (2010). Parasympathetic innervation maintains epithelial progenitor cells during salivary organogenesis. Science *329*, 1645-1647.

Lombaert, I.M., Brunsting, J.F., Wierenga, P.K., Faber, H., Stokman, M.A., Kok, T., Visser, W.H., Kampinga, H.H., de Haan, G., and Coppes, R.P. (2008a). Rescue of salivary gland function after stem cell transplantation in irradiated glands. PLoS One *3*, e2063.

Lombaert, I.M., Brunsting, J.F., Wierenga, P.K., Kampinga, H.H., de Haan, G., and Coppes, R.P. (2008b). Cytokine treatment improves parenchymal and vascular

damage of salivary glands after irradiation. Clin Cancer Res *14*, 7741-7750.

Lombaert, I.M., Wierenga, P.K., Kok, T., Kampinga, H.H., deHaan, G., and Coppes, R.P. (2006). Mobilization of bone marrow stem cells by granulocyte colony-stimulating factor ameliorates radiation-induced damage to salivary glands. Clin Cancer Res *12*, 1804-1812.

Maimets, M., Bron, R., de Haan, G., van Os, R., and Coppes, R.P. (2015). Similar ex vivo expansion and post-irradiation regenerative potential of juvenile and aged salivary gland stem cells. Radiother Oncol *116*, 443-448.

Maimets, M., Rocchi, C., Bron, R., Pringle, S., Kuipers, J., Giepmans, B.N., Vries, R.G., Clevers, H., de Haan, G., van Os, R*., et al.* (2016). Long-Term In Vitro Expansion of Salivary Gland Stem Cells Driven by Wnt Signals. Stem Cell Reports *6*, 150-162.

Marg, A., Escobar, H., Gloy, S., Kufeld, M., Zacher, J., Spuler, A., Birchmeier, C., Izsvak, Z., and Spuler, S. (2014). Human satellite cells have regenerative capacity and are genetically manipulable. J Clin Invest *124*, 4257-4265.

Maria, O.M., Maria, A.M., Cai, Y., and Tran, S.D. (2012). Cell surface markers CD44 and CD166 localized specific populations of salivary acinar cells. Oral Dis *18*, 162-168.

Mishima, K., Inoue, H., Nishiyama, T., Mabuchi, Y., Amano, Y., Ide, F., Matsui, M., Yamada, H., Yamamoto, G., Tanaka, J*., et al.* (2012). Transplantation of side population cells restores the function of damaged exocrine glands through clusterin. Stem Cells *30*, 1925-1937.

Nanduri, L.S., Baanstra, M., Faber, H., Rocchi, C., Zwart, E., de Haan, G., van Os, R., and Coppes, R.P. (2014). Purification and ex vivo expansion of fully functional salivary gland stem cells. Stem Cell Reports *3*, 957-964.

Nanduri, L.S., Maimets, M., Pringle, S.A., van der Zwaag, M., van Os, R.P., and Coppes, R.P. (2011). Regeneration of irradiated salivary glands with stem cell marker expressing cells. Radiother Oncol *99*, 367-372.

Neumann, Y., David, R., Stiubea-Cohen, R., Orbach, Y., Aframian, D.J., and Palmon, A. (2012). Long-term cryopreservation model of rat salivary gland stem cells for future therapy in irradiated head and neck cancer patients. Tissue Eng Part C Methods *18*, 710-718.

Ng, A., Tan, S., Singh, G., Rizk, P., Swathi, Y., Tan, T.Z., Huang, R.Y., Leushacke, M., and Barker, N. (2014). Lgr5 marks stem/progenitor cells in ovary and tubal epithelia. Nat Cell Biol *16*, 745-757.

Notta, F., Doulatov, S., Laurenti, E., Poeppl, A., Jurisica, I., and Dick, J.E. (2011). Isolation of single human hematopoietic stem cells capable of long-term multilineage engraftment. Science *333*, 218-221.

Ohyama, M., Terunuma, A., Tock, C.L., Radonovich, M.F., Pise-Masison, C.A., Hopping, S.B., Brady, J.N., Udey, M.C., and Vogel, J.C. (2006). Characterization and isolation of stem cell-enriched human hair follicle bulge cells. J Clin Invest *116*, 249-260.

Osailan, S.M., Proctor, G.B., McGurk, M., and Paterson, K.L. (2006). Intraoral duct ligation without inclusion of the parasympathetic nerve supply induces rat submandibular gland atrophy. Int J Exp Pathol *87*, 41-48.

Pellegrini, G., Traverso, C.E., Franzi, A.T., Zingirian, M., Cancedda, R., and De Luca, M. (1997). Long-term restoration of damaged corneal surfaces with autologous cultivated corneal epithelium. Lancet *349*, 990-993.

Pringle, S., Van Os, R., and Coppes, R.P. (2013). Concise review: Adult salivary gland stem cells and a potential therapy for xerostomia. Stem Cells *31*, 613-619.

Reynolds, B.A., and Weiss, S. (1992). Generation of neurons and astrocytes from isolated cells of the adult mammalian central nervous system. Science *255*, 1707-1710.

Rugel-Stahl, A., Elliott, M.E., and Ovitt, C.E. (2012). Ascl3 marks adult progenitor cells of the mouse salivary gland. Stem Cell Res *8*, 379-387.

Sato, A., Okumura, K., Matsumoto, S., Hattori, K., Hattori, S., Shinohara, M., and Endo, F. (2007). Isolation, tissue localization, and cellular characterization of progenitors derived from adult human salivary glands. Cloning Stem Cells *9*, 191-205.

Sato, T., and Clevers, H. (2013). Growing self-organizing mini-guts from a single intestinal stem cell: mechanism and applications. Science *340*, 1190-1194.

Schuijers, J., and Clevers, H. (2012). Adult mammalian stem cells: the role of Wnt, Lgr5 and R-spondins. EMBO J *31*, 2685-2696.

Shackleton, M., Vaillant, F., Simpson, K.J., Stingl, J., Smyth, G.K., Asselin-Labat, M.L., Wu, L., Lindeman, G.J., and Visvader, J.E. (2006). Generation of a functional mammary gland from a single stem cell. Nature *439*, 84-88.

Smyth, G.K., Michaud, J., and Scott, H.S. (2005). Use of within-array replicate spots for assessing differential expression in microarray experiments. Bioinformatics *21*, 2067-2075.

Takahashi, S., Shinzato, K., Domon, T., Yamamoto, T., and Wakita, M. (2004). Mitotic proliferation of myoepithelial cells during regeneration of atrophied rat submandibular glands after duct ligation. J Oral Pathol Med *33*, 430-434.

Vissink, A., Burlage, F.R., Spijkervet, F.K., Jansma, J., and Coppes, R.P. (2003a). Prevention and treatment of the consequences of head and neck radiotherapy. Crit Rev Oral Biol Med *14*, 213-225.

Vissink, A., Jansma, J., Spijkervet, F.K., Burlage, F.R., and Coppes, R.P. (2003b). Oral sequelae of head and neck radiotherapy. Crit Rev Oral Biol Med *14*, 199-212.

Xiao, N., Lin, Y., Cao, H., Sirjani, D., Giaccia, A.J., Koong, A.C., Kong, C.S., Diehn, M., and Le, Q.T. (2014). Neurotrophic factor GDNF promotes survival of salivary stem cells. J Clin Invest *124*, 3364-3377.

Yui, S., Nakamura, T., Sato, T., Nemoto, Y., Mizutani, T., Zheng, X., Ichinose, S., Nagaishi, T., Okamoto, R., Tsuchiya, K*., et al.* (2012). Functional engraftment of colon epithelium expanded in vitro from a single adult Lgr5(+) stem cell. Nat Med *18*, 618-623.